Current Biology *18*, 1227–1233, August 26, 2008 ©2008 Elsevier Ltd All rights reserved DOI 10.1016/j.cub.2008.07.042

Report

A Dynamin-Related Protein Required for Nuclear Remodeling in *Tetrahymena*

Abdur Rahaman,[1] Nels C. Elde,[2] and Aaron P. Turkewitz[1,*]
[1]Department of Molecular Genetics and Cell Biology
The University of Chicago
920 E. 58th Street
Chicago, Illinois 60637
[2]Division of Basic Sciences
Fred Hutchinson Cancer Research Center
Seattle, Washington 98109

Summary

Dynamin-related proteins (DRPs) are GTPases that reversibly assemble on cellular membranes [1]. Individual DRPs (here "DRP" includes authentic dynamins) function in fission or tubulation of the plasma membrane, trans-Golgi network, mitochondria, peroxisomes, chloroplasts, and endosomes [1] and in mitochondrial fusion [2]. Many of these functions are widespread; they are present in animals, plants, trypanosomes, Giardia, ciliates, alga, and slime molds [3–8]. Lineage-specific expansions of the gene family created specialized DRPs. In animals, such DRPs include MxB, which has been reported to regulate nuclear-pore transport [9]. Whereas many unicellular organisms possess a small number of DRPs, expansions occurred in some protist lineages. The eight DRPs in the ciliate *Tetrahymena thermophila* might contribute to aspects of ciliate complexity. Each ciliate cell contains distinct germline and somatic nuclei, whose differentiation and maintenance must require distinct machinery [10, 11]. Here we show that Drp6p, previously shown to be targeted to the nuclear envelope [3], is required for macronuclear development. Drp6p activity, which is distinct from that of the only other known nuclear DRP, is modulated by a combination of stage-specific subcellular targeting and assembly dynamics. This work demonstrates a novel DRP activity and presents a system in which environmental and developmental cues can be used for manipulating key aspects of regulation.

Results

A Lineage-Specific and Recently Evolved Clade of DRPs in *Tetrahymena*

The eight *T. thermophila* DRPs each possesses three canonical domains (GTPase, middle, and GTPase effector). Similarity between Drp6p and classical dynamin, including residues involved in GTP binding and hydrolysis, is shown in Figures S1A and S1B in the Supplemental Data available online. *DRP6* is related (~59% amino acid identity) to *DRP3–5.* The four loci are adjacent on macronuclear chromosome CH670412 (http://www.ciliate.org/). The cluster is phylogenetically isolated from the other four *T. thermophila* DRPs (Figure S1C). In addition, no other sequenced protist genome, including that of the ciliate *Paramecium tetraurelia* (Figure S1D), encodes a DRP that falls into the *DRP3-6* clade. We also queried a large EST library from *Ichthyophthirius multifiliis*, the ciliate most closely related to *T. thermophila*, for which genome-scale data are currently available. Although *Ichthyophthirius* DRPs related to *T. thermophila DRP1*, *2*, *7*, and *8* were easily identified (our unpublished data), none related to *DRP3–6* was found. Therefore, this set of DRPs in *T. thermophila* represents a family of relatively new genes. The unusual localization of Drp6p to the nuclear envelope hinted at convergent evolution in that this localization is shared with MxB in animals. We therefore asked whether Drp6p and MxB have similar functions.

Drp6p Is Not a Protist MxB

Each *Tetrahymena* cell contains a polyploid transcriptionally active macronucleus (mac) and a diploid, silent germline micronucleus (mic). Two different tagged variants of Drp6p (GFP-*drp6-4* and HA-*drp6-1*) localized at or near the envelopes of both nuclei in growing cells (Figures 1A and 1B). Both tagged forms also appeared as cytoplasmic puncta that also bore features of the endoplasmic reticulum (Figure S2). The transcript of the *drp6-4* transgene, integrated at the *MTT1* locus, was ~14-fold more abundant than the low level of the endogenous *DRP6* transcript (not shown). Although such overexpression carries the risk of spurious localization, it was necessary because we could not detect the Drp6p expressed at the low endogenous level. Reassuringly, individual cells showed a wide range of GFP-drp6-4p expression, and mac, mic, and cytoplasmic signals were seen even in cells with the lowest visible expression levels. We also caution that HA-Drp6p and GFP-Drp6p, like tagged DRPs in most systems, do not appear to be fully active proteins (see details below). To ask whether Drp6p is enriched at nuclear-pore complexes (NPC), we coexpressed HA-drp6-1p together with a GFP-tagged NPC component, Nup3p (from D. Chalker, Washington University). GFP-nup3p was diffuse throughout the mac envelope in both living (not shown) and fixed (Figure 1C and Figure S3B) cells. HA-drp6-1p on the same nuclei was patchily distributed and showed little colocalization with Nup3-GFP. GFP-drp6-4p in living cells showed a similar patchy distribution, distinct from that of Nup3p (Figures S3A and S3B). We asked whether Nup3p targeting depended on the presence of Drp6p by generating Δ*DRP6* cell lines lacking all mac alleles of *DRP6* (Figures S3C and S3D). Δ*DRP6* cells were viable and showed a wild-type distribution of GFP-nup3p (Figure S3E). We saw no differences by electron microscopy between wild-type and Δ*DRP6* in the nuclear-envelope ultrastructure of cryofixed cells.

Unlike MxB, *DRP6* does not appear to be involved in transport of nuclear localization sequence (NLS)-targeted proteins. GFP expressed in wild-type *Tetrahymena* distributed throughout the cytosol and mac, as expected because GFP can diffuse passively through NPCs [12] (Figure 1D). However, when an NLS was added to GFP, the protein was concentrated within the mac. Importantly, we obtained the same result when NLS-GFP was localized in Δ*DRP6* cells. This result does not appear to be due to functional redundancy of Drp6p with Drp3p, 4p or 5p because none of these related DRPs, expressed as GFP-tagged constructs, localized to nuclei (not

*Correspondence: apturkew@uchicago.edu

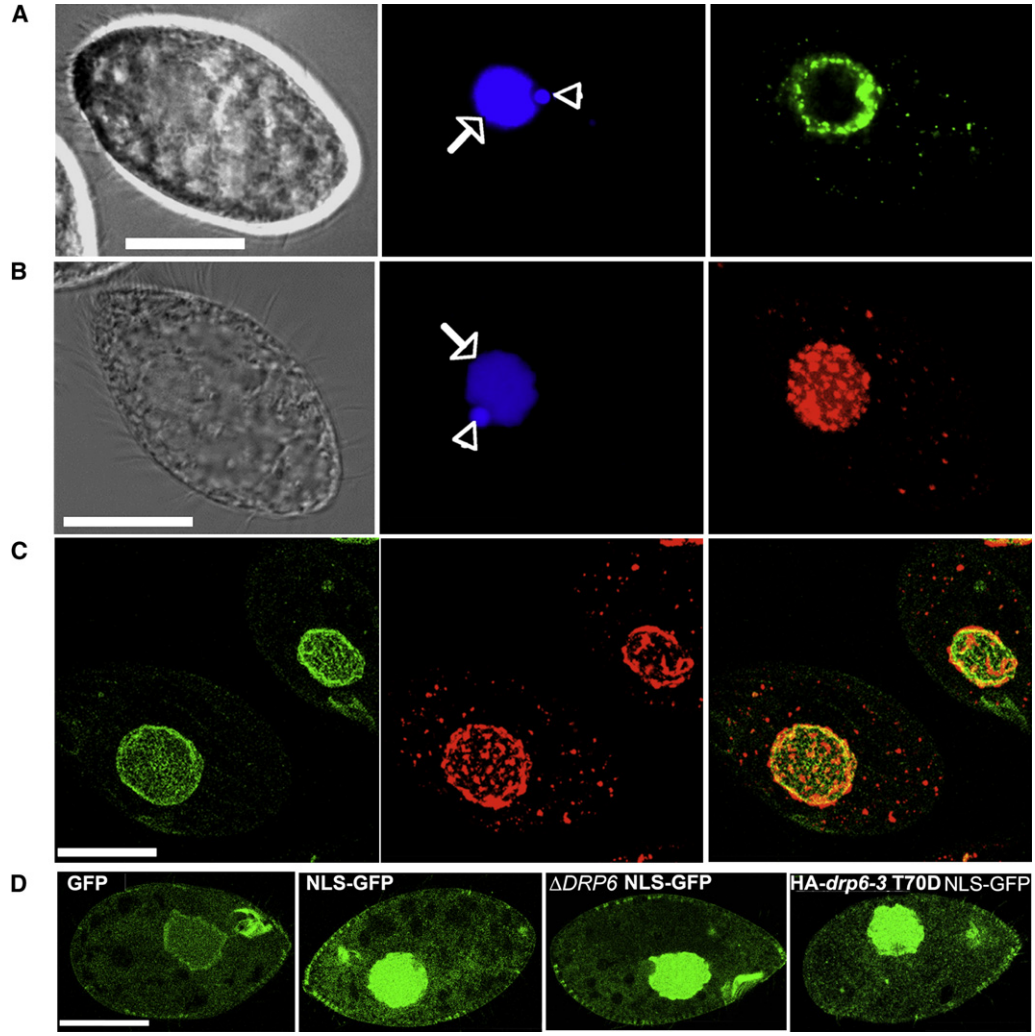

Figure 1. Drp6p Localizes to Nuclear Envelopes but Is Not Essential for Nuclear Import

(A) Left: phase-contrast image of fixed growing cell. Center: DAPI-stained mac (arrow) and mic (arrowhead). Right: GFP-drp6-4p is at the periphery of both nuclei and in cytoplasmic puncta. The scale bar represents 20 μM.

(B) Left: phase-contrast image of fixed growing cell. Center: DAPI-stained nuclei. Right: HA-drp6-1p visualized by indirect immunofluorescence and shown as a confocal stack. The scale bar represents 20 μM.

(C) Confocal stacks of cells coexpressing GFP-nup3p and HA-drp6-1p. GFP-nup3p is diffuse throughout the mac envelope (left), whereas HA-drp6-1p is in discrete patches (middle). The merged image is at the right. GFP-nup3p is also seen at the oral apparatus and at the cortex. The scale bar represents 20 μM.

(D) Wild-type or Δ*DRP6* cells or cells expressing HA-*drp6-3* T70D were transformed to express either GFP or GFP with a C-terminal nuclear localization signal (GFP-NLS). Confocal micrographs of fixed cells are shown. GFP-NLS accumulated strongly in nuclei of wild-type, Δ*DRP6*, and HA-*drp6-3* T70D cells.

shown). Further evidence that Drp6p is not involved in nuclear import came from cells expressing HA-*drp6-3* T70D, representing a substitution of aspartic acid for threonine 70, a conserved residue critical for efficient GTP hydrolysis in other DRPs (Figure S1B). In particular, the corresponding mutation in MxB inhibited nuclear import [9]. Although the inducible expression of HA-*drp6-3* T70D in *Tetrahymena* did generate other phenotypes (below), it did not affect transport of NLS-GFP (Figure 1D). These data indicate that Drp6p, though targeted to the nuclear envelope like MxB, plays a distinct role not previously documented for a DRP.

A Role for *DRP6* in Nuclear Differentiation

Starved *Tetrahymena* cells become competent for conjugation (Figure 2A) [13]. After pair formation between cells of complementary mating types, the mic in each cell undergoes elongation ("crescent formation"). Micronuclear meiosis produces haploid gametes that are exchanged between paired cells before fusing to form new pronuclei. Pronuclei divide and subsequently differentiate into two new mics and two developing macs (anlagen) in each cell. During this period, each cell also retains the old mac, which begins to degenerate 12 hr after pair formation. These nuclear events occur synchronously in mated wild-type cells and have been extensively studied with respect to chromosome rearrangements, but nothing is known about mechanisms underlying the implied restructuring of nuclear membranes.

The *DRP6* transcript could be detected in vegetative cells and became somewhat less abundant in starvation (not shown). Peak expression of *DRP6* occurred in conjugating pairs 8 hr after mixing, suggesting a role at this stage (Figure 2B). We therefore asked whether *DRP6* were specifically required for any stage in conjugation. Note that *DRP6* in conjugants can be transcribed both from the parental macs and,

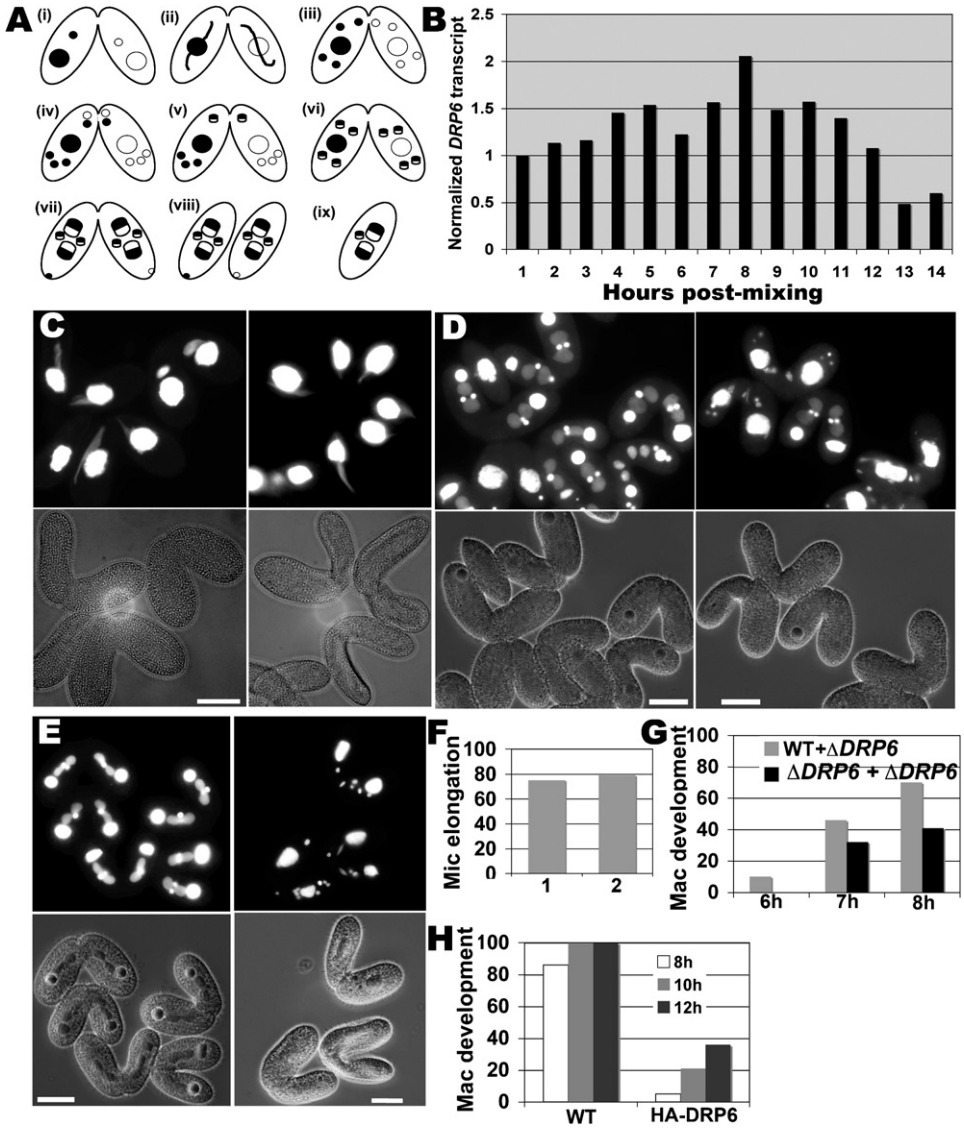

Figure 2. *DRP6* Is Required for Macronuclear Development

(A) Conjugation stages in *Tetrahymena*. (i) pair formation, (ii) crescent stage (3 hr after mixing), (iii) meiosis (4.5 hr after mixing), (iv) pronuclear exchange (5 hr), (v) pronuclear fusion (5.5 hr), (vi) second postzygotic mitosis (6.5 hr), (vii) new mac development (8 hr), (viii) pair separation (12 hr) and (ix) mac resorption and mic degradation (16 hr).

(B) Starved cultures of two complementary mating types were mixed, and RNA samples were isolated subsequently. *DRP6* mRNA in each sample, determined by reverse transcription PCR, was normalized with respect to α-tubulin mRNA. Maximum expression occurs 8 hr after mixing, corresponding to mac development.

(C) Δ*DRP6* cells were crossed with the wild-type (left) or with a complementary Δ*DRP6* strain (right). Pairs fixed at 3 hr were visualized by phase-contrast (lower panel) or DAPI-fluorescence (upper panel). Mic elongation, equivalent in both crosses, is quantified in (F) (1 = wild-type × Δ*DRP6*; 2 = Δ*DRP6* × Δ*DRP6*; n = 100–150).

(D) Same as (C) but fixed 8 hr after mixing. Most conjugants in the Δ*DRP6* × wild-type crosses show two developing macs in each partner (left), whereas developing macs are only present in a minority of the Δ*DRP6* × Δ*DRP6* pairs (right). Results are quantified in (G) for pairs fixed at 6, 7, and 8 hr (n = 150–200).

(E) A wild-type strain expressing endogenous *DRP6* was crossed either with a second wild-type strain or with cells transformed to also overexpress HA-*drp6-1*. Pairs were fixed at 8 hr and visualized as in (C). Most wild-type × wild-type pairs show two developing macs in each partner (left), whereas developing macs are seen in a minority of pairs in which one partner expresses HA-*drp6-1* (right). The scale bar represents 20 μM. Results are quantified in (H) for pairs fixed at 8, 10, and 12 hr (n = 150–200).

starting at ~8 hr, from the newly developing macs. Eliminating all *DRP6* transcription in conjugants therefore requires disruption of all mic and mac alleles, but we were unable to disrupt *DRP6* in the mic. We therefore took two complementary approaches to analyze *DRP6* function during conjugation. First, we generated two Δ*DRP6* (mac) strains with complementary mating types and set up pairings of Δ*DRP6* × Δ*DRP6*, Δ*DRP6* × wild-type, and wild-type × wild-type. The latter two were indistinguishable, but Δ*DRP6* × Δ*DRP6* conjugants had clear stage-specific nuclear defects. Mic elongation (Figures 2C and 2F) and meiosis (Figure S4) were unaffected, but the appearance of developing macs at 8 hr was ~2-fold inhibited (Figures 2D and 2G). The lack of complete inhibition could be accounted for by transcription from the intact *DRP6*

alleles in the new macs developing at that stage. Consistent with this, overexpression from the inducible *MTT1* promoter in conjugants of tagged *DRP6* alleles, or of GTP-binding or hydrolysis mutants, resulted in dominant-negative inhibition of mac development starting at 8 hr (Figures 2E and 2H; Figure S5) [14]. Because overexpression of the epitope-tagged wild-type allele and the GTPase mutants gave similar results, we do not know whether the latter were acting in a classical dominant-negative fashion. The inhibition by any of these constructs persisted so that few cells developed visible new macs even in conjugation endpoints (Figures S5 and S6). The defect was gene-specific because it was not recapitulated by comparable overexpression of tagged *DRP3–5* (Figure S7). Conjugants expressing *DRP6* transgenes were also defective in a subsequent step, the active degrading of parental macs at ~12 hr (Figure S6). Transcription from the new mac is required for this step, so persistence of the parental macs in pairs expressing *DRP6* transgenes can be considered an indirect result of the inability to build new macs [15].

Localization studies provided important support for a direct role of *DRP6* in mac formation. At early stages in conjugation, GFP-drp6-4p (or HA-drp6-1p) did not decorate nuclei but instead localized to cytoplasmic puncta (Figure 3A). However, beginning at ~8 hr, Drp6p associated strongly with the nuclear envelopes (Figure 3B). For the minority of GFP-drp6-4p-expressing mating pairs that proceeded to stage viii as shown in Figure 2A, Drp6p was still associated with the developing macs as well as the mics (Figure 3C). Thus, the targeting of Drp6p to nuclear membranes is stage specific during conjugation. It is also nucleus specific; a consistent feature was that HA-drp6-4p clearly failed to reassociate with the parental mac, normally destined for degradation (Figure 3B). Taken together, the results indicate that Drp6p plays a specific role in conjugation and that this role is likely to be exerted most directly at the stage of mac development.

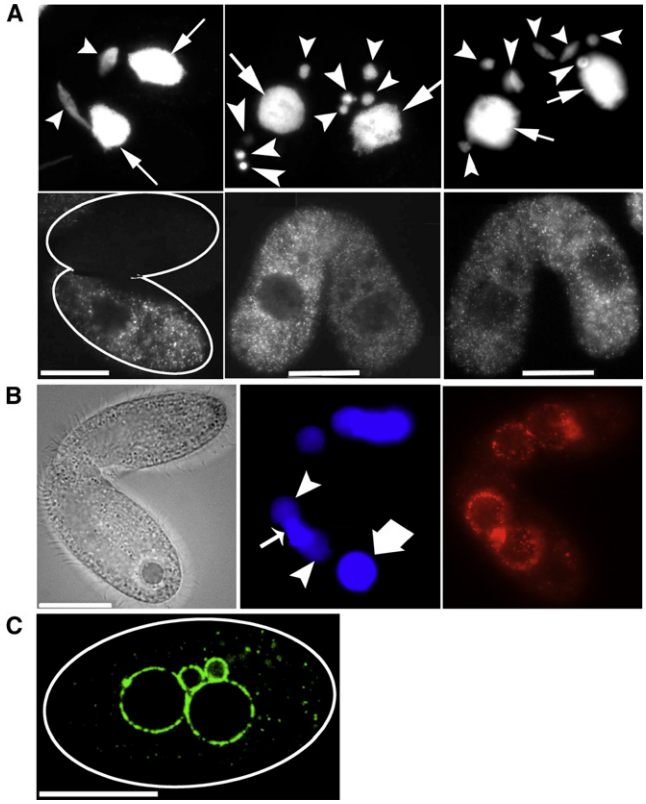

Figure 3. Drp6p Localization in Conjugating Cells

(A) (left) Pair in which one partner is expressing GFP-drp6-4p, as viewed 3 hr after mixing. (Top) DAPI-stained nuclei. (Bottom) GFP-drp6-4p is largely restricted to the expressing cell and is dispersed in cytoplasmic puncta. (Middle and right panels) Pairs, with one cell expressing GFP-drp6-4p, at the pronuclear selection stage (see Figure 2A, iii). (Top) DAPI-stained mics (arrowheads) and macs (arrows). (Bottom) GFP-drp6-4p is dispersed.

(B) Pair in which one partner is expressing HA-drp6-1p, as viewed 9 hr after mixing. (Left) Phase-contrast. (Middle) DAPI-stained old parental mac (thick arrow); developing macs (solid arrowheads); mic (thin arrow) (note: a second mic is not visible in this plane). The developing macs at this stage have a lower ploidy than the old mac and thus stain less brightly. (right) HA-drp6-1p, visualized by indirect immunostaining, is targeted to developing macs and the mic, but not to the old mac.

(C) A cell expressing GFP-drp6-4p, derived from a mating pair at 16 hr after mixing. GFP-drp6-4p is localized to both mics and newly developed macs and in cytoplasmic puncta. The scale bar represents 20 μM.

DRP6 Activity during Vegetative Growth

DRP6 may be required for rapid nuclear-envelope expansion that occurs during mac development in conjugants. Nuclear-envelope expansion also occurs during the vegetative cell cycle, and *DRP6* transcript levels in elutriation-synchronized vegetative cultures (RNA was generously provided by D. Romero, U. Minnesota) peaked shortly after cell division, a period when cells enter macronuclear S phase (Figure S8). Δ*DRP6* cells grew slowly (Figure S9A) and accumulated excess DNA (Figure S9B). These defects were also observed in transformants expressing *DRP6* transgenes, including GTP-binding and -hydrolysis mutants (Figures S9A and S9C). The defects were specific because strains bearing the NEO3 cassette at other loci (for example, Δ*GRL6*) or bearing the same construct to overexpress other proteins (for example, GFP-*rab36*) showed no comparable growth inhibition (Figure S9A). Thus, like developing macs in conjugating cells, nuclei in growing cells depend upon *DRP6* function, albeit less critically.

Drp6p Is Activated in Starved and Conjugating Cells

Drp6p associates with nuclei in growing cells but dissociates during early conjugation and then reassociates with selected nuclei at later stages. Drp6p in starved, nonconjugating cells showed an intermediate localization, with clear nuclear targeting but also prominent cytoplasmic puncta (Figure S10). The localization of DRPs, like that of many cytoplasmic proteins, is dynamic rather than static; it depends on GTP-fueled rounds of assembly and disassembly, which drive the protein's association and dissociation from target membranes. We used FRAP (fluorescence recovery after photobleaching) to confirm that GFP-Drp6p localization was dynamic. For comparison, we also analyzed GFP-tagged Drp1p, a DRP involved in clathrin-mediated endocytosis [3]. GFP-drp1-1p in growing cells showed rapid exchange, and fluorescence recovered in photobleached spots after ~2 min (Figures 4A and 4B). In contrast, GFP-drp6-4p showed very slow recovery (Figures 4A and 4B). Similarly slow rates were seen at either the mac or mic (not shown). Strikingly, the mobility of Drp6p increased dramatically upon starvation and in fact became roughly equivalent to that of Drp1p (Figures 4C and 4D). Drp6p mobility was equally high when measured by initial bleaching of either the mac or the mic. Drp6p was also highly mobile in starved conjugating cells at the 8 hr stage, when the protein is targeted to nuclear membranes. The changes in mobility are likely to reflect modulation of Drp6p assembly and/or disassembly at the nuclear envelope.

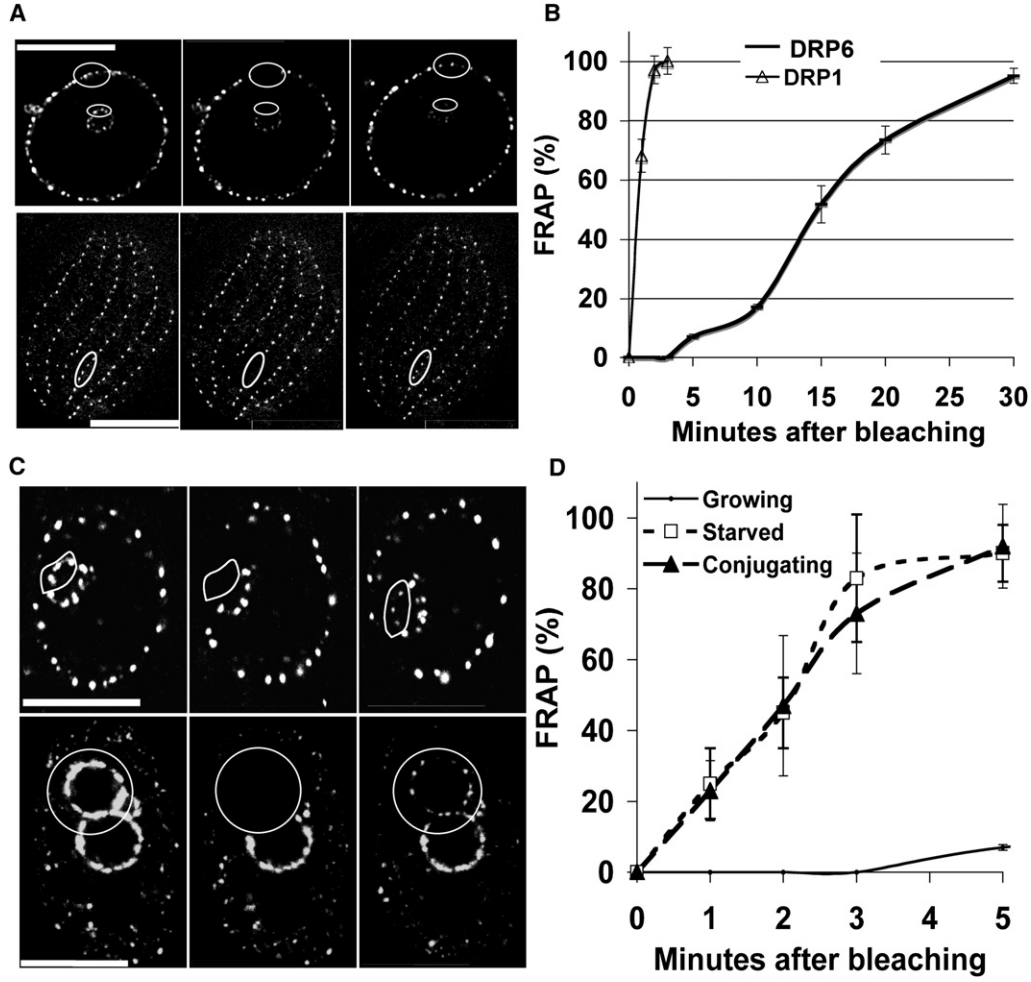

Figure 4. Drp6p Is Activated in Starved and Conjugating Cells

(A) FRAP in growing cells of GFP-drp6-4p and GFP-drp1-1p. The upper panel focuses on the nuclei within a cell expressing GFP-drp6-4p; the oval is the area of the mac to be photobleached. The second frame shows the cell immediately after photobleaching. The nuclei 30 min after bleaching appear in the third frame. The scale bar represents 10 μM. FRAP of nuclear GFP-drp6-4p in growing cells is quantified (for n = 3) in panels (B) and (D). Lower panel: GFP-drp1-1p is present at regularly spaced endocytic sites, whose distribution along cortical rows in a single cell is shown. The zone to be photobleached is shown by an oval. The cell immediately after bleaching appears in the second frame, and at 2 min after bleaching in the third frame. FRAP is quantified for GFP-drp1-1p in growing cells (n = 3) in panel (B). The scale bar represents 20 μM.

(C) FRAP of GFP-drp6-4p in a starved cell (upper panel) and in an exconjugant (lower panel). The distributions of GFP-drp6-4p on the respective nuclei are shown in the left panels, and the areas to be photobleached are outlined. The second frames show the nuclei immediately after photobleaching. The recovering signals 2 min after bleaching are shown in the third frame. The upper panel shows photobleaching of Drp6p in the mic; identical results were obtained for photobleaching of mac-localized Drp6p. FRAP results for starved and conjugating cells are quantified (for n = 3) in panel (D). Similar FRAP results were obtained in exconjugant cells.

Error bars in (B) and (D) represent standard deviations.

Discussion

As shown in this paper, a recently evolved DRP in *T. thermophila* has acquired a novel function at the nuclear envelope. Drp6p is targeted primarily to both mac and mic envelopes, and some protein was also found in cytoplasmic puncta that appeared to be long-lived and mobile in continuous imaging of live cells. These may be comparable to vesicular forms of ER of unknown function in higher plants [16]. Further work will be required if we are to investigate their potential functional significance and confirm that active Drp6p, expressed at endogenous levels, is targeted to these bodies.

The activity of Drp6p is clearly different from that of the sole previously characterized nuclear-envelope DRP, MxB in animals, which by some unknown mechanism regulates import at nuclear pores. In contrast, neither null nor variant alleles of *DRP6* interfered with accumulation of NLS-GFP in growing cells. It remains possible that *DRP6* shifts its function to nuclear transport in starved or conjugating cells. We consider this unlikely, but for technical reasons such cells could not be assayed for NLS-GFP import. Our results instead suggest that Drp6p facilitates specific nuclear-membrane dynamics. The most dramatic *DRP6*-dependent phenotypes were seen during conjugation, but the gene also plays a function in vegetative cultures. The number of *DRP6* transcripts in growing cells shows cell-cycle periodicity and peaks during macronuclear S phase. *DRP6* is essential for rapid vegetative growth, a striking result because the gene evolved only recently and might be restricted to the *Tetrahymena* lineage. The growth defect was seen in Δ*DRP6* cells and was even more acute in

cells expressing a *DRP6* variant that no longer binds to the nuclear envelope. Similar alleles of DRPs result in dominant inhibition in other systems [6, 17]. Whether the *DRP6* variants act via a classical dominant-negative mechanism in *Tetrahymena* is not yet clear because we found that many *DRP6* phenotypes could be recapitulated by simple overexpression of tagged *DRP6* alleles. We could not study expression of these tagged alleles at the level of the endogenous gene because not enough *DRP6* is transcribed.

Both the absence of *DRP6* (Δ*DRP6*) and Drp6p overexpression resulted in dramatic nuclear defects during conjugation. Although our data cannot yet define a precise site of action for Drp6p, there are strong hints. *DRP6* mRNA peaks at 8 hr after conjugation begins. At this stage, but not in previous stages, Drp6p is targeted to nuclei, specifically the new mics and developing macs. Strikingly, a large fraction of such macs failed to develop in cells where parental Drp6p was absent, or when tagged or mutated alleles were overexpressed. These defects were specific for *DRP6* because mac formation was not comparably inhibited by overexpression of related *DRPs*. One possibility is that Drp6p, like a subset of mitochondrial DRPs, functions to promote membrane fusion [2, 18]. At the mac envelope, fusion with compatible vesicles or tubules could fuel membrane expansion. It is intriguing that Drp6p is not required for crescent elongation, a step requiring expansion of the mic envelope [19]. The difference between crescent mics and developing macs in their dependence on *DRP6* suggests that *Tetrahymena* use more than one mechanism of nuclear-envelope expansion.

All GTPases are regulated by interaction with GTPase-activating proteins (GAPs). For DRPs, the GAP activity resides on the same polypeptide as the GTPase domain. These domains interact *in trans* when the protein self-assembles, thereby linking oligomerization, localization, and GTP turnover [20]. The activity of DRPs can also be regulated by post-translational modification. This is well illustrated for the DRP involved in mitochondrial scission, Drp1 [21, 22]. Although specific residues and their posttranslational modifications, as well as associated mitochondrial phenotypes, have been identified, it is less clear whether or how those modifications affect the Drp1 assembly/disassembly cycle, GTPase activity, or localization.

Tetrahymena Drp6p represents a striking example of a novel role for DRPs and also offers a clear case of physiological regulation at multiple levels. First is regulation of transcript abundance during the cell cycle and particularly during conjugation. Second, Drp6p shows at least three stage-specific patterns of localization. The protein is targeted to the nuclear envelope in growing cells, but it dissociates when cells are starved so that a large proportion of Drp6p shifts to cytoplasmic puncta. This shift is exacerbated when starved cells are mated, such that Drp6p is no longer visibly associated with nuclear envelopes at early stages in conjugation. Subsequently, the protein reassociates strongly with the new mics and the developing macs, but not with the parental macs. The last aspect of Drp6p regulation is that recycling of the GFP-tagged protein at nuclear envelopes, as measured by FRAP, increases dramatically in starved or conjugating cells compared to vegetative cells. We hypothesize that posttranslational Drp6p modifications, linked to changes in metabolism and conjugation, are modulating the GTPase activity to control the assembly/disassembly cycle. Since starvation as well as conjugation can be easily synchronized in *Tetrahymena*, this offers a highly accessible system for probing mechanisms involved in DRP regulation.

Supplemental Data

Supplemental Experimental Procedures and ten figures are available with this article online at http://www.current-biology.com/cgi/content/full/18/16/1227/DC1/.

Acknowledgments

For valuable reagents we thank D. Romero (University of Minnesota), D. Chalker (Washington University, St. Louis), and M. Gorovsky and J. Bowen (University of Rochester, NY); for sharing gene expression data we thank W. Miao and M. Gorovsky (University of Rochester, NY); for other help we thank E. Cole (St. Olaf College, MN), C. Jahn (Northwestern University Medical School, Chicago), J. Frankel (University of Iowa) and members of this laboratory: N. Khuong, L. Bright, N. Kambesis, and M. Zampa. We received EM help from Jotham Austin II (University of Chicago) and Tom Giddings, Alex Stemm-Wolf, and Mark Winey (University of Colorado, Boulder). Light microscopy was done at the Integrated Light Microscopy Core Facility (University of Chicago); flow cytometry was done at the Cancer Research Center Facility (University of Chicago). N.C.E. is an Ellison Medical Foundation Fellow of the Life Sciences Research Foundation. This work was supported by National Science Foundation grant NSF-MCB-0422011 and National Institutes of Health grant GM077607 to A.P.T.

Received: March 25, 2008
Revised: July 8, 2008
Accepted: July 10, 2008
Published online: August 14, 2008

References

1. Praefcke, G.J., and McMahon, H.T. (2004). The dynamin superfamily: Universal membrane tubulation and fission molecules? Nat. Rev. Mol. Cell Biol. *5*, 133–147.
2. Meeusen, S., DeVay, R., Block, J., Cassidy-Stone, A., Wayson, S., McCaffery, J.M., and Nunnari, J. (2006). Mitochondrial inner-membrane fusion and crista maintenance requires the dynamin-related GTPase Mgm1. Cell *127*, 383–395.
3. Elde, N.C., Morgan, G., Winey, M., Sperling, L., and Turkewitz, A.P. (2005). Elucidation of Clathrin-mediated endocytosis in Tetrahymena reveals an evolutionarily convergent recruitment of Dynamin. PLoS Genet *1*, e52.
4. Segui-Simarro, J.M., Austin, J.R., 2nd, White, E.A., and Staehelin, L.A. (2004). Electron tomographic analysis of somatic cell plate formation in meristematic cells of Arabidopsis preserved by high-pressure freezing. Plant Cell *16*, 836–856.
5. Wienke, D.C., Knetsch, M.L., Neuhaus, E.M., Reedy, M.C., and Manstein, D.J. (1999). Disruption of a dynamin homologue affects endocytosis, organelle morphology, and cytokinesis in Dictyostelium discoideum. Mol. Biol. Cell *10*, 225–243.
6. Gaechter, V., Schraner, E., Wild, P., and Hehl, A.B. (2008). The single dynamin family protein in the primitive protozoan giardia lamblia is essential for stage conversion and endocytic transport. Traffic *9*, 57–71.
7. Chanez, A.L., Hehl, A.B., Engstler, M., and Schneider, A. (2006). Ablation of the single dynamin of T. brucei blocks mitochondrial fission and endocytosis and leads to a precise cytokinesis arrest. J. Cell Sci. *119*, 2968–2974.
8. Nishida, K., Takahara, M., Miyagishima, S.Y., Kuroiwa, H., Matsuzaki, M., and Kuroiwa, T. (2003). Dynamic recruitment of dynamin for final mitochondrial severance in a primitive red alga. Proc. Natl. Acad. Sci. USA *100*, 2146–2151.
9. King, M.C., Raposo, G., and Lemmon, M.A. (2004). Inhibition of nuclear import and cell-cycle progression by mutated forms of the dynamin-like GTPase MxB. Proc. Natl. Acad. Sci. USA *101*, 8957–8962.
10. Collins, K., and Gorovsky, M.A. (2005). Tetrahymena thermophila. Curr. Biol. *15*, R317–R318.
11. Li, S., Yin, L., Cole, E.S., Udani, R.A., and Karrer, K.M. (2006). Progeny of germ line knockouts of ASI2, a gene encoding a putative signal transduction receptor in Tetrahymena thermophila, fail to make the transition from sexual reproduction to vegetative growth. Dev. Biol. *295*, 633–646.
12. Terry, L.J., Shows, E.B., and Wente, S.R. (2007). Crossing the nuclear envelope: Hierarchical regulation of nucleocytoplasmic transport. Science *318*, 1412–1416.

13. Martindale, D.W., Allis, C.D., and Bruns, P.J. (1982). Conjugation in Tetrahymena thermophila. A temporal analysis of cytological stages. Exp. Cell Res. *140*, 227–236.
14. Shang, Y., Song, X., Bowen, J., Corstanje, R., Gao, Y., Gaertig, J., and Gorovsky, M.A. (2002). A robust inducible-repressible promoter greatly facilitates gene knockouts, conditional expression, and overexpression of homologous and heterologous genes in Tetrahymena thermophila. Proc. Natl. Acad. Sci. USA *99*, 3734–3739.
15. Ward, J.G., and Herrick, G. (1996). Effects of the transcription inhibitor actinomycin D on postzygotic development of Tetrahymena thermophila conjugants. Dev. Biol. *173*, 174–184.
16. Staehelin, L.A. (1997). The plant ER: a dynamic organelle composed of a large number of discrete functional domains. Plant J. *11*, 1151–1165.
17. van der Bliek, A.M., Redelmeier, T.E., Damke, H., Tisdale, E.J., Meyerowitz, E.M., and Schmid, S.L. (1993). Mutations in human dynamin block an intermediate stage in coated vesicle formation. J. Cell Biol. *122*, 553–563.
18. Mozdy, A.D., and Shaw, J.M. (2003). A fuzzy mitochondrial fusion apparatus comes into focus. Nat. Rev. Mol. Cell Biol. *4*, 468–478.
19. Wolfe, J., Hunter, B., and Adair, W.S. (1976). A cytological study of micronuclear elongation during conjugation in Tetrahymena. Chromosoma *55*, 289–308.
20. Muhlberg, A.B., Warnock, D.E., and Schmid, S.L. (1997). Domain structure and intramolecular regulation of dynamin GTPase. EMBO J. *16*, 6676–6683.
21. Harder, Z., Zunino, R., and McBride, H. (2004). Sumo1 conjugates mitochondrial substrates and participates in mitochondrial fission. Curr. Biol. *14*, 340–345.
22. Cribbs, J.T., and Strack, S. (2007). Reversible phosphorylation of Drp1 by cyclic AMP-dependent protein kinase and calcineurin regulates mitochondrial fission and cell death. EMBO Rep. *8*, 939–944.